Synthesis conditions and real structure of $Sr_{n+1}Ti_nO_{3n+1}$ oxides.

Boreskov Institute of Catalysis

Novosibirsk State University

*THE REAL SCIENCE

Gorkusha A.S.[1,2*], Pavlova S.N.[2], Ivanova Y.A.[2], Gerasimov E.Y.[2], Isupova L.A.[2], Tsybulya S.V.[1,2]

[1]Novosibirsk State University; [2]Boreskov Institute of Catalysis SB RAS;

*deepforesttt922@gmail.com; +79526058081

Introduction

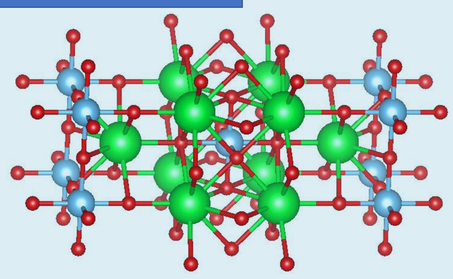

$A_{n+1}B_nO_{3n+1}$

- A (Ca, Ba, Sr)
- B (Ti, Sn)
- Oxygen

Solid oxide fuel cells.
$La_{n+1}Ni_nO_{3n+1}$ (n = 1 - 3)

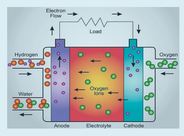

Yatoo, M.A.; Skinner, S.J. Mater. Today Proc. 2022, 56, 3747–3754.

Thermoelectrics
$Sr_2Ti_{1-x}Nb_xO_4$ (n = 1, 2)

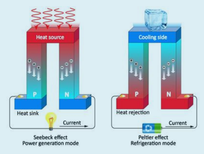

Lee, K.H.; Kim, S.W. J. Appl. Phys. 2006, 100, 063717.

Ruddlesden-Popper (R-P) structures are layered perovskite-like oxides with the general formula $A_{n+1}B_nO_{3n+1}$ (A=Ca, Ba, Sr, B=Ti, Sn). At present, these structures are being actively studied as promising materials for various photocatalysts, solid oxide fuel cells, thermoelectronics, etc.

In particular, the $Sr_{n+1}Ti_nO_{3n+1}$ systems are considered as a potential material for a catalyst for the oxidative coupling of methane (OCM). At present, to obtain fuels from natural gas, indirect synthesis methods are used with an intermediate stage of syngas production carried out at high temperature and pressure. More rational methods seem to be direct methods for converting methane into useful products, among which the OCM reaction for the production of ethane and ethylene (C2) is promising. However, the industrial use of OCM is difficult due to the insufficient yield of C2 hydrocarbons on the studied simple and mixed oxides, as well as their low stability. Thus, the development of new OCM oxide catalysts with high activity, selectivity, and stability is an urgent problem, and fundamental research is being carried out in many laboratories around the world to solve it.

In this work, we studied the effect of synthesis conditions and the composition of initial reagents on the formation of layers of perovskite-like oxides $Sr_{n+1}Ti_nO_{3n+1}$ (n = 1 – 3), as well as on the real structure of these systems. Also in this work, a method was proposed for determining the content of planar defects in the A_2BO_4 structure from powder diffraction data.

Oxidative coupling of methane

Traditional methods

$CH_4 + O_2$; H_2O; CO_2

↓

$CO + H_2$ (syngas)

↓

Liquid fuel
C_xH_y, $C_xH_yO_z$

Many stages
High pressure

OCM:

$CH_4 + O_2$

↓

Liquid fuel
C_xH_y, $C_xH_yO_z$

One stage
Atmosphere pressure

Sr_2TiO_4

Sample 1 – starting materials: $SrCO_3$ + TiO_2. Mechanochemical activation: **APF-5** low-energy mill; 10 minutes; iron drums; zirconia balls. Calcination at 1100 °C.
Sample 2 - starting materials : $SrCO_3$ + TiO_2. Mechanochemical activation: **AGO-2** high-energy mill; 20 minutes; iron drums; zirconia balls. Calcination at 1100 °C [1].

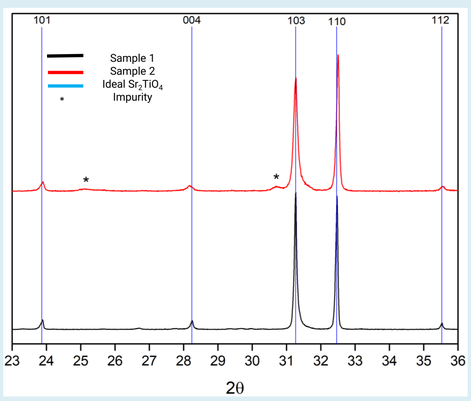

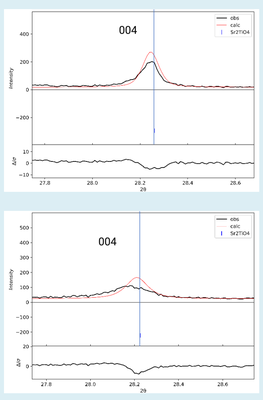

Figure 1

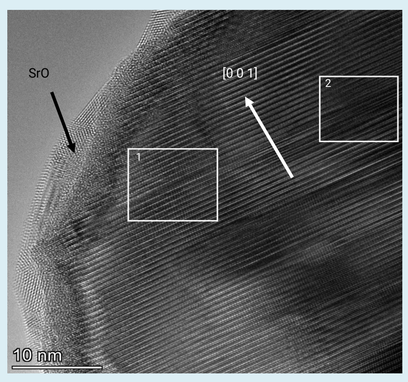

Figure 2

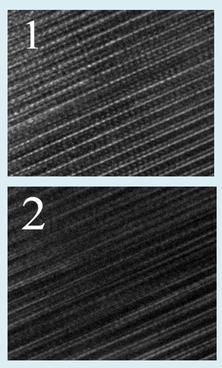

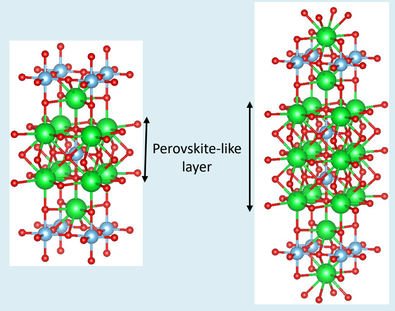

Figure 3

According to X-ray phase analysis, Sample 1 and Sample 2 are single-phase Sr_2TiO_4. However, a more detailed comparison of X-ray (fig. 1) diffraction patterns shows that they are not completely identical: the experimental positions of some reflections do not coincide to varying degrees with the positions of the same reflections in the ideal structure of Sr_2TiO_4 [ICSD-194719]. This discrepancy may be due to the presence of some disorder in the structure.

This assumption is confirmed by high-resolution transmission electron microscopy data (fig. 2) – multiple planar defects are observed in the bulk of the samples, which violate the periodicity in the alternation of layers in the 001 direction.

The existence of this kind of defect can be explained by the fact that within the framework of the Ruddlesden-Popper structural series, there are similar crystal structures that differ from each other in the length of the perovskite-like layer (fig. 3). The presence of such similar structural elements gives grounds to assume that fragments with one or two alternating perovskite-like layers can quite simply form in the volume of particles.

Using the calculation of diffraction patterns from one-dimensionally disordered structures [2], we simulated the effect of such defects on the diffraction patterns of Sr_2TiO_4 [3]. Reflections with a nonzero index *l* are displaced to varying degrees relative to their positions in the defect-free structure (fig. 4), while reflections of the *hk0* type are not displaced.

Based on this effect, we proposed a method for estimating the content of planar defects in structures of the A_2BO_4 type: using relation (1), using the values of interplanar distances for reflections 004, 103, and 110, we can calculate parameter Δ, which can be used to determine the content of defects according to the graph (fig.5).

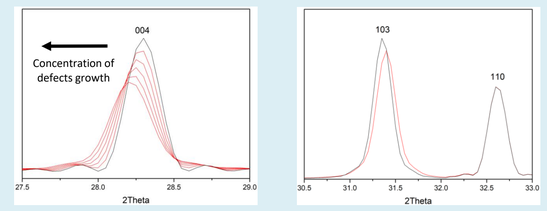

Figure 4

Black – defect-free structure.
Red color - defective structures (δ = 0 – 0.01).

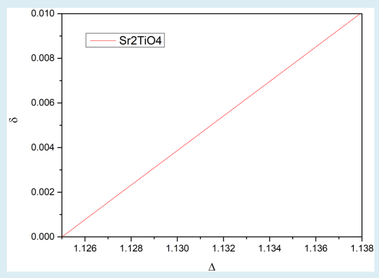

Figure 5

The chemical composition for a particular parameter. δ:
$(0.5 - δ)/(0.5 + δ)SrO + SrTiO_3$ (1)

For sample 1 δ = 0.002 => $Sr_{1.99}TiO_{3.99}$

For sample 2 δ = 0.004 => $Sr_{1.98}TiO_{3.98}$

$Sr_3Ti_2O_7$ and $Sr_4Ti_3O_{10}$

All samples were obtained using the solid-phase synthesis method with the stage of preliminary mechanochemical activation – $SrCO_3$ + TiO_2 in stoichiometric ratios; APF-5; 12 minutes; iron drums; zirconia balls. Calcination at 1100 and 1300 °C.

Phase composition				
Sample	$Sr_3Ti_2O_7$	$Sr_3Ti_2O_7$	$Sr_4Ti_3O_{10}$	$Sr_4Ti_3O_{10}$
Calcination temperature, °C	1100	1300	1100	1300
$Sr_3Ti_2O_7$	100	100	28	30
$SrTiO_3$	-	-	72	70

Table 1

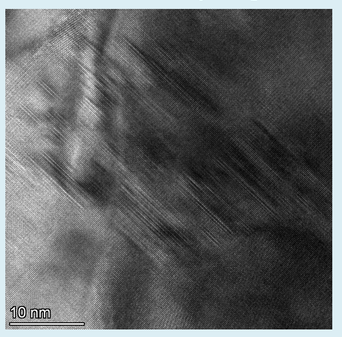

Figure 1

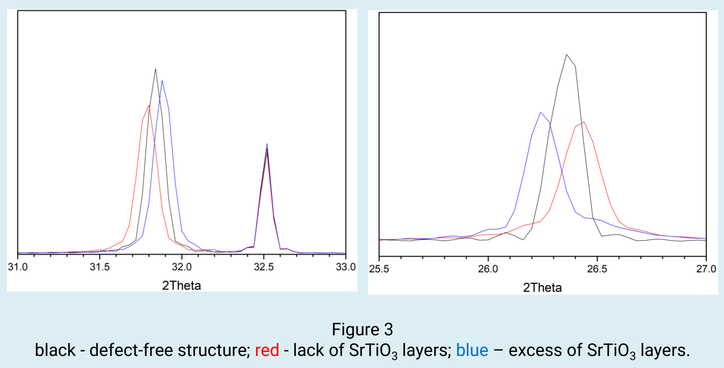

Figure 3

black - defect-free structure; red - lack of $SrTiO_3$ layers; blue – excess of $SrTiO_3$ layers.

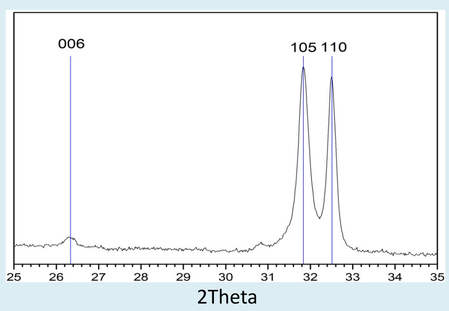

Figure 4

Lack of layers $SrTiO_3$
$SrO + (2-δ(SrTiO_3))$

Defect-free structure
$SrO + 2(SrTiO_3)$

Excess layers $SrTiO_3$
$SrO + (2+δ(SrTiO_3))$

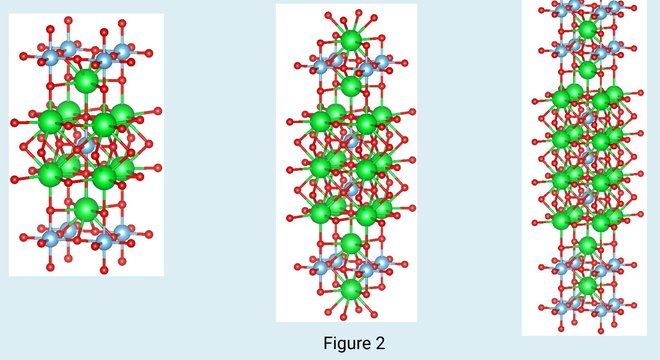

Figure 2

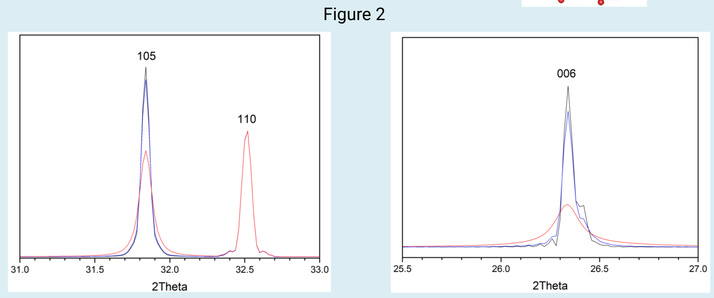

Figure 5

black - defect-free $Sr_3Ti_2O_7$; red - 10% of defects of each type; blue - 1% of defects of each type;.

Within the framework of this work, it was also interesting to refine the procedure for the synthesis of the higher members of the Ruddlesden-Popper series, $Sr_3Ti_2O_7$ and $Sr_4Ti_3O_{10}$. As can be seen from Table 1, it was possible to obtain single-phase $Sr_3Ti_2O_7$ at different calcination temperatures. It was not possible to obtain the $Sr_4Ti_3O_{10}$ phase under the given synthesis conditions. Next, we studied the $Sr_3Ti_2O_7$ sample calcined at 1100°C.

By analogy with Sr_2TiO_4, it was assumed that $Sr_3Ti_2O_7$ may also contain planar defects. High-resolution transmission electron microscopy confirmed this assumption (Fig. 1).

However, within this system, several types of defects can simultaneously exist: fragments can form both with a lack of perovskite-like layers and with their excess (Fig. 2).

We have simulated the influence of such defects on the diffraction patterns of $Sr_3Ti_2O_7$. Within the framework of this simulation, we used 2 extreme cases – a lack of 10% SrTiO3 layers and an excess of SrTiO3 layers. As can be seen from Fig. 3, in the case of a lack of perovskite-like layers, as well as in the case of an excess of these layers, the position of reflections with non-zero indices l shifts to a different extent, and the position of reflections with zero indices *l* remains unchanged for any change in the content of $SrTiO_3$ layers. It is also interesting to note that both types of defects lead to a shift in the positions of the same reflections in opposite directions by equal values of 2Θ (with the same content of defects).

Powder X-ray diffraction data (Fig. 4) show that the experimental positions of the diffraction maxima are in good agreement with the theoretically calculated positions of the same maxima for the defect-free $Sr_3Ti_2O_7$ system, which is inconsistent with the HRTEM data (Fig. 1). Therefore, we performed additional simulations to evaluate the case in which both types of defects simultaneously exist in the system.

As can be seen from Fig. 5, the positions of all reflections really remain unchanged at the same content of planar defects in the structure. It is also seen that the widths of the diffraction maxima change with an increase in the defect content: in the case of a defective structure, reflections with a nonzero index *l* are noticeably wider than reflections of the *hk*0 type. Such an effect is actually observed in the experimental diffraction pattern of the $Sr_3Ti_2O_7$ sample (Fig. 4) — it can be seen with the naked eye that the 105 reflection is much wider than the 110 reflection. However, it is too early to draw any conclusions at the moment, and the $Sr_3Ti_2O_7$ system requires further research.

Conclusion

- Single-phase samples of $Sr_{n+1}Ti_nO_{3n+1}$ (n = 1, 2) were synthesized by the solid-phase synthesis method with the stage of mechanochemical activation and high-temperature calcination.
- The sample with n = 3 could not be synthesized under the given synthesis conditions
- The influence of planar defects (violating stoichiometry) on the diffraction patterns of $Sr_{n+1}Ti_nO_{3n+1}$ (n = 1, 2) was simulated.
- A technique has been developed for determining the content of planar defects for A_2BO_4 structures.

References

[1] Pavlova, S. et al. *Catalysts* **2022**
[2] Cherepanova, S. V., Tsybulya, S. V. Materials Science Forum **2004**.
[3] Gorkusha, A. et al. *Materials* **2022**